Research Article | Vol. 28, No. 2 / 20 January 2020 / Optics Express 1316
Optics EXPRESS

Multipartite quantum entanglement creation for distant stationary systems

TAO LI,[1,*] ZHENKAI WANG,[2,3] AND KEYU XIA[2,3,4,5]

[1]School of Science, Nanjing University of Science and Technology, Nanjing 210094, China
[2]National Laboratory of Solid State Microstructures, Collaborative Innovation Center of Advanced Microstructures, Nanjing University, Nanjing 210093, China
[3]College of Engineering and Applied Sciences, and School of Physics, Nanjing University, Nanjing 210093, China
[4]Jiangsu Key Laboratory of Artificial Functional Materials, and Key Laboratory of Intelligent Optical Sensing and Manipulation, Ministry of Education, Nanjing University, Nanjing 210093, China
[5]keyu.xia@nju.edu.cn
*Tao.Li@njust.edu.cn

Abstract: We present efficient protocols for creating multipartite Greenberger-Horne-Zeilinger (GHZ) and W states of distant stationary qubits. The system nonuniformity and/or the non-ideal single-photon scattering usually limit the performance of entanglement creation, and result in the decrease of the fidelity and the efficiency in practical quantum information processing. By using linear optical elements, errors caused by the system nonuniformity and non-ideal photon scattering can be converted into heralded loss in our protocols. Thus, the fidelity of generated multipartite entangled states keeps unchanged and only the efficiency decreases. The GHZ state of distant stationary qubits is created in a parallel way that its generation efficiency considerably increases. In the protocol for creating the W state of N distant stationary qubits, an input single photon is prepared in a superposition state and sent into N paths parallelly. We use the two-spatial-mode interferences to eliminate the "which path" single-photon scattering "knowledge". As a result, the efficiency of creating the N-qubit W state is independent of the number of stationary qubits rather than exponentially decreases.

1. Introduction

Quantum entanglement is one of the cornerstones at the foundation of quantum mechanics and plays an important role in various quantum technologies, such as distributed quantum computation [1–4], quantum key distribution [5–7], quantum teleportation [8], and quantum secure direct communication [9–14]. Despite the creation of entanglement between two particles has been well developed, the creation of multipartite entanglement becomes exceedingly difficult for systems with many particles [15–23]. To generate entanglement between two distant stationary qubits, it usually needs a flying photonic qubit as a mediate entangling with a stationary qubit [24–26], in combination with the quantum swapping or quantum interference [27–30]. The entanglement between the stationary and flying qubits significantly limits the available entanglement between two distant stationary qubits [31–33]. Furthermore, this limitation usually becomes more serious for the creation of multipartite entanglement.

Multipartite entanglement demonstrates distinct power to reveal the non-classicality of quantum physics [15,34,35] and to perform many important quantum protocols in which more than two parties come together [36,37]. The GHZ and W states are two typical classes of multipartite entangled states that cannot be converted to each other by stochastic local operations and classical communications. The GHZ states violate Bell inequalities maximally and exhibit a remarkable property for error-tolerant quantum computation and multiparty quantum networks [38–43]. Meanwhile, these GHZ states are extremely fragile due to particle loss. In contrast, the W-state

#383152 https://doi.org/10.1364/OE.383152
Journal © 2020 Received 14 Nov 2019; revised 25 Dec 2019; accepted 26 Dec 2019; published 8 Jan 2020

Optics EXPRESS

entanglement is maximally persistent and robust against particle loss [44–46]. Therefore, the W states may lead to stronger non-classicality than GHZ states, and play important roles in quantum information processing [47–52].

The creation of multipartite entanglement, especially the GHZ and W states, attracts much attention as a result of their distinct applications for quantum technologies. For photonic systems, the creation of the GHZ and W states are mainly implemented by quantum fusion that consists of quantum interference and post-selection operations [15,53,54]. The creation of GHZ entanglement among distant stationary systems are usually implemented by a cascaded extension of schemes for entangling two stationary qubits [55–59], where the hybrid photon-qubit entanglement between a photon and a stationary qubit plays a central role. Any deviation from the ideal condition for the creation of hybrid entanglement will accumulate to considerably limit the creation of the target state when the number of qubits increases [55–59]. Furthermore, the creation of the W state can also be implemented by using hybrid entanglement between a photon and a stationary qubit in combination with multi-path optical interferences and post-selection operations [60–65]. Another promising method for creating multipartite entanglement among stationary qubits uses a data bus that simultaneously interacts with all stationary qubits [66–71]. A proper control on this system cannot only create a GHZ state but also create a W state [66–71]. The number of qubits in the reported GHZ and W states is still small even using the state-of-the-art technology of coupling stationary qubits with a common data bus [72].

Here we propose two efficient protocols for the creation of multipartite entanglement among stationary qubits. In the first protocol, we describe a parallel method for the creation of a four-stationary-qubit GHZ state using the error-rejecting scattering of a single photon, involving a cavity or waveguide that couples to a stationary qubit [26,27]. A click of single-photon detectors heralds the creation of GHZ entanglement among distant stationary qubits. The errors involved in a practical single-photon scattering process are passively picked out and thus only cause the decrease of the success efficiency other than its fidelity. In the second protocol, we present an efficient method for the creation of W states of four stationary qubits. This protocol involves only one effective single-photon scattering process and significantly decreases the requirement of the phase stability, since two-spatial-mode interferences are used to replace the multi-spatial-mode interference [60–65]. The errors introduced by the deviation from ideal scattering conditions are also suppressed by passive filtering. Furthermore, the extension of both methods to larger numbers of particles are straightforward. Therefore, our protocols may promise applications in various multipartite-entanglement-based quantum tasks, i.e., quantum networks and quantum computation.

2. Single-photon and single-spin interface

A single-photon and single-spin interface serves as a key resource to create hybrid entanglement and thus is a key ingredient for distributed quantum computation as well as for multiparty quantum networks. An 1D cavity- or waveguide-emitter system provides an efficient interface between single photons and emitters [73–88]. Single photons impinging into such system will be scattered into a channel that in principle depends on the state of the emitter. We consider a singly-charged self-assembled In(Ga)As quantum dot (QD) that is coupled to a single-sided micropillar cavity [73–76]. Due to the Pauli's exclusion principle, the optical transition between the ground state $|\uparrow\rangle$ ($|\downarrow\rangle$) and the negatively charged trion X^- state $|\uparrow\downarrow\Uparrow\rangle$ ($|\uparrow\downarrow\Downarrow\rangle$) is accompanied by the absorption of a right-circularly (left-circularly) polarized photon $|R\rangle$ ($|L\rangle$), but either cross transition is forbidden [89]. Furthermore, the two dipole-allowed transmissions are degenerated when the environment magnetic field is zero, as shown in Fig. 1. Here the spin-quantization axis is along the growth direction of the QD and in parallel with the direction of the input photon.

When a circularly-polarized photon with a frequency ω impinges into a system consisting of a single-sided micropillar cavity and a QD, it will be either reflected or absorbed due to the cavity

Optics EXPRESS

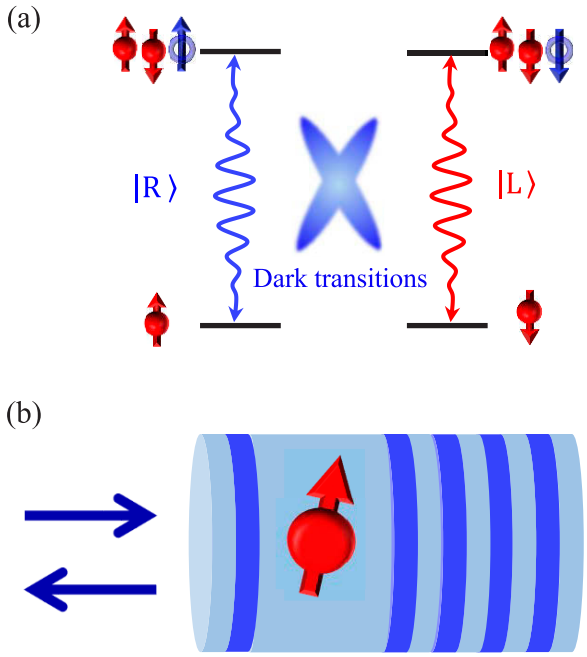

Fig. 1. Schematic diagram of spin-dependent transitions for a negatively-charged exciton X^-. (a) Four-level structure and optical transition of a negatively-charged quantum dot (QD); (b) a QD coupled to a single-sided micropillar cavity. Here, two ground states $|\uparrow\rangle$ and $|\downarrow\rangle$ denote the electron-spin states with J_z equal to $\pm 1/2$; $|\uparrow\downarrow\Uparrow\rangle$ and $|\uparrow\downarrow\Downarrow\rangle$ denote two trion states of X^- with $J_z = \pm 3/2$. The dipole transition $|\uparrow\rangle \leftrightarrow |\uparrow\downarrow\Uparrow\rangle$ ($|\downarrow\rangle \leftrightarrow |\uparrow\downarrow\Downarrow\rangle$) is optically driven by a right- (left-) circularly-polarized photon $|R\rangle$ ($|L\rangle$). Therefore, the cross transitions (dark transitions) are forbidden by the quantum-optical selection rules.

mode loss. This process can be studied with the quantum-jump approach [90]. The dissipative time evolution is described by an effective Hamiltonian ($\hbar = 1$) [27,28]

$$\hat{H}_{eff} = (\Delta_- - \frac{i\gamma}{2})\hat{\sigma}_+\hat{\sigma}_- + (\Delta_c - \frac{i\kappa_s}{2})\hat{a}^\dagger\hat{a} + ig(\hat{a}\hat{\sigma}_+ - \hat{a}^\dagger\hat{\sigma}_-). \tag{1}$$

Here the non-Hermitian terms account for additional decay mechanisms of an excited QD-cavity system, i.e., the cavity mode $\hat{a}$ and the QD exciton X^- decay into nondirectional channels at rates κ_s and γ, respectively. $\Delta_- = \omega_- - \omega$ and $\Delta_c = \omega_c - \omega$ are the detunings, where ω_c and ω_- are frequencies of the cavity mode and the X^- transition, respectively. Meanwhile, g represents the coupling strength between the cavity mode and the QD. Although the evolution of our system described by the Hamiltonian $\hat{H}_{eff}$ can be interrupted by random quantum jumps [27,28,90], we are interested in the dynamics including a single photon that projects the system into a Hilbert space without quantum jumps: an input photon is scattered into the reflection mode of the QD-cavity system and leads to a click of one single-photon detector in entanglement-creation setups.

The reflection coefficient for such a system can be obtained by solving dynamical equations for the cavity field operator $\hat{a}$ and dipole operator $\hat{\sigma}_-$,

$$\begin{aligned} \frac{d\hat{a}}{dt} &= -[i\Delta_c + \frac{\kappa + \kappa_s}{2}]\hat{a} - g\hat{\sigma}_- - \sqrt{\kappa}\,\hat{a}_{in}, \\ \frac{d\hat{\sigma}_-}{dt} &= -[i\Delta_- + \frac{\gamma}{2}]\hat{\sigma}_- - g\hat{\sigma}_z\,\hat{a}. \end{aligned} \tag{2}$$

Optics EXPRESS

Here κ describes the input coupling rate between the cavity mode and input/output mode. For simplicity, the frequency ω_- is tuned to be identical to ω_c, leading to an identical detuning $\Delta_- = \Delta_c = \Delta$. In combination with the input-output theory $\hat{a}_{out} = \hat{a}_{in} + \sqrt{\kappa}\,\hat{a}$, one can obtain the reflection coefficient [75–77,91],

$$r(\Delta, g) = \frac{[i\Delta + \frac{\gamma}{2}][i\Delta + \frac{\kappa_s - \kappa}{2}] + g^2}{[i\Delta + \frac{\gamma}{2}][i\Delta + \frac{\kappa + \kappa_s}{2}] + g^2}. \tag{3}$$

Here $\Delta = \omega_c - \omega$ is the detuning between the input photon and the cavity mode. When the input photon is in a polarization state that does not couple to the QD, i.e., $g = 0$, the reflection coefficient is changed into

$$r(\Delta, 0) = \frac{i\Delta + \frac{\kappa_s - \kappa}{2}}{i\Delta + \frac{\kappa + \kappa_s}{2}}, \tag{4}$$

which is significantly different from $r(\Delta, g)$ that is obtained when the input photon couples to the QD. We will show below that increasing the difference $|r(\Delta, g) - r(\Delta, 0)|$ promises a higher efficiency for the creation of multipartite entanglement.

In general, the absolute values of $r(\Delta, 0)$ and $r(\Delta, g)$ are less than unity due to the finite absorption of the cavity and/or the decay of an excited QD. When an input photon in a circularly polarized state i.e., $|R\rangle$ is scattered by a QD-cavity system, in which the QD is initialized to a superposition state $|\psi\rangle = \alpha|\uparrow\rangle + \beta|\downarrow\rangle$ ($|\alpha|^2 + |\beta|^2 = 1$), the state of the QD and the photon evolves into $|\psi'\rangle = |R\rangle[r(\Delta, g)\alpha|\uparrow\rangle + r(\Delta, 0)\beta|\downarrow\rangle]/\sqrt{p_0}$ with a probability $p_0 = |r(\Delta, g)\alpha|^2 + |r(\Delta, 0)\beta|^2$, provided the photon is scattered into the reflection mode and no quantum jump happens [75–77,91]. Particularly, when a linearly polarized photon $|H\rangle = (|R\rangle + |L\rangle)/\sqrt{2}$ or $|V\rangle = (|R\rangle - |L\rangle)/\sqrt{2}$ is impinging into the cavity-QD system with the QD in a state $|\pm\rangle = (|\uparrow\rangle \pm |\downarrow\rangle)/\sqrt{2}$, the hybrid system consisting of the single photon and the QD evolves as follows

$$\begin{aligned} |H\rangle|\pm\rangle &\rightarrow \frac{1}{\sqrt{p_1}}[R_+|H\rangle|\pm\rangle + R_-|V\rangle|\mp\rangle], \\ |V\rangle|\pm\rangle &\rightarrow \frac{1}{\sqrt{p_1}}[R_-|H\rangle|\mp\rangle + R_+|V\rangle|\pm\rangle], \end{aligned} \tag{5}$$

where the parameters $R_\pm = [r(\Delta, g) \pm r(\Delta, 0)]/2$, and $p_1 = [|r(\Delta, g)|^2 + |r(\Delta, 0)|^2]/2$ represents the probability that the linearly-polarized photon is scattered into the reflection mode. Therefore, after a single-photon scattering process, the hybrid system evolves into a hybrid entangled state that consists of two orthogonal components: (1) the QD and the photon are both unchanged with a probability $|R_+|^2$; (2) the QD and the photon are both flipped, while the corresponding probability is $|R_-|^2$. The first component usually corresponds to a trivial scattering result that is referred to as error for simplicity, and can be passively filtered out using linear optical elements, while the second component constitutes a fascinating building block for quantum information processing, such as the creation of GHZ and W states of many spatially separated QDs.

3. Proposals for quantum entanglement creation

In this section, we describe two individual setups for creating GHZ and W states, as shown in Fig. 2 and 3. The errors caused by the non-ideal single-photon scattering are passively filtered out by polarizing beam splitters (PBSs), where all QD-cavity systems are assumed to be identical [51,55–58,81].

3.1. Creation of GHZ entanglement among four distant QDs

The main idea for the creation of four-QD GHZ state exploits the aforementioned single-photon and single-spin interface. A parallel schematic setup for the creation is shown in Fig. 2. It is

Optics EXPRESS

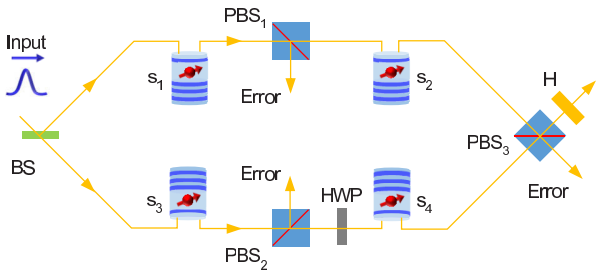

Fig. 2. Schematic diagram of the four-QD GHZ-state creation. Here BS denotes a 50/50 beam splitter that transmits and reflects a photon equally. PBS_i (i=1, 2, and 3) denotes a polarizing beam splitter that transmits (reflects) photons in the linearly-polarized state $|H\rangle$ ($|V\rangle$). HWP and H are two half-wave plates that are respectively tuned to apply the bit-flip operation and the Hadamard transformation, i.e., $|H\rangle \rightarrow (|H\rangle + |V\rangle)/\sqrt{2}$ or $|V\rangle \rightarrow (|H\rangle - |V\rangle)/\sqrt{2}$ on photons passing them.

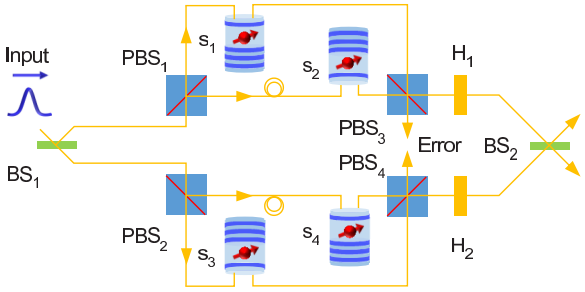

Fig. 3. Schematic diagram of the four-QD W-state creation. Here BS_1 and BS_2 denote two 50/50 beam splitters that transmit and reflect a photon equally. PBS_i (i =1, 2, 3, and 4) denotes a polarizing beam splitter that transmits (reflects) photons in the linearly-polarized state $|H\rangle$ ($|V\rangle$). H_1 and H_2 are two half-wave plates that apply the Hadamard transformation, i.e., $|H\rangle \rightarrow (|H\rangle + |V\rangle)/\sqrt{2}$ or $|V\rangle \rightarrow (|H\rangle - |V\rangle)/\sqrt{2}$ on photons passing them.

composed of four QD-cavity systems with each QD in the state $|+\rangle$ and linear optical elements, i.e., a 50/50 beam splitter (BS), PBSs, and half-wave plates (HWP or H). HWP is tuned to apply a bit-flip operation on photons passing it, while H is arranged to complete the Hadamard transformation, i.e., $|H\rangle \rightarrow \frac{1}{\sqrt{2}}(|H\rangle + |V\rangle)$ or $|V\rangle \rightarrow \frac{1}{\sqrt{2}}(|H\rangle - |V\rangle)$. The PBS transmits photons in the state $|H\rangle$ and reflects photons in the state $|V\rangle$. QD-cavity systems in different spatial modes of the BS evolve differently when a photon with the polarization $|V\rangle$ impinges into the setup. After filtering out errors, the elimination of optical paths in which the single photon passes will project the four QDs into $|\mathrm{GHZ}^+\rangle$ or $|\mathrm{GHZ}^-\rangle$ with $|\mathrm{GHZ}^\pm\rangle = \frac{1}{\sqrt{2}}(|++--\rangle \pm |--++\rangle)$, where the phase is determined by the polarization of the output photon.

For a photon $|V\rangle$ impinging on the BS, it is either reflected or transmitted by the BS. If the photon is in the reflection mode, it will be reflected by QD s_1 that is coupled to a microcavity. The PBS_1 passively filters out the error component with the photon in the state $|V\rangle$ and passes the useful component with the photon in the state $|H\rangle$ to impinge on another microcavity that contains QD s_2. However, if the photon is in the transmission mode, it will be reflected by the microcavity containing QD s_3. The error scattering component with the output photon in the state $|V\rangle$ is filtered out by PBS_2. The correct scattering component suffers a bit-flip operation by passing the photon through the HWP. The photon then impinges on the microcavity that contains the QD s_4. The evolutions of the transmission and reflection modes take place simultaneously.

Optics EXPRESS

Therefore, before the photon passes through the PBS_3, the system consisting of the photon and four QDs evolves into a non-normalized state

$$\begin{aligned}|\Psi_1\rangle = R_-\big(|V_R\rangle|-\rangle_{s_1}|-\rangle_{s_2}|+\rangle_{s_3}|+\rangle_{s_4} + |H_T\rangle|+\rangle_{s_1}|+\rangle_{s_2}|-\rangle_{s_3}|-\rangle_{s_4}\big)\\ + R_+\big(|H_R\rangle|-\rangle_{s_1}|+\rangle_{s_2}|+\rangle_{s_3}|+\rangle_{s_4} + |V_T\rangle|+\rangle_{s_1}|+\rangle_{s_2}|-\rangle_{s_3}|+\rangle_{s_4}\big).\end{aligned} \tag{6}$$

where the subscript R (T) denotes that the photon is in the reflection (transmission) mode of the BS; the subscripts s_i with $i = 1, 2, 3, 4$ represent four different QDs. Note the optical path difference between two individual modes has been tuned to zero [81], otherwise it introduces a relative phase proportional to it in the longer mode. The two components with the photon in the state $|H\rangle_R$ and $|V\rangle_T$ will be passively filtered out and lead to errors that can be detected by placing a single-photon detector in the lower output mode of PBS_3.

The first two terms of Eq. (6) indicate a five-qubit GHZ state, consisting of four QDs and one flying photon. The half-wave plate H in the upper output mode of PBS_3 completes a Hadamard operation on the photon and evolves the system into

$$|\Psi_2\rangle = \frac{1}{\sqrt{2}}\big(|V\rangle|\mathrm{GHZ}^-\rangle + |H\rangle|\mathrm{GHZ}^+\rangle\big). \tag{7}$$

A measurement of the single photon in the linearly-polarized basis $\{|H\rangle, |V\rangle\}$ disentangles the photon from QDs and projects the four QDs into the GHZ state $|\mathrm{GHZ}^+\rangle$ ($|\mathrm{GHZ}^-\rangle$) when the outcome of the measurement is $|H\rangle$ ($|V\rangle$).

The extension of the method to create GHZ states of larger numbers (N) of QDs is straightforward. When N is even, we can divide QDs equally into two subgroups and place each $N/2$ QDs in a cascaded way similar to that shown in Fig. 2. However, when N is odd, we can divide QDs into two subgroups of numbers $(N-1)/2$ and $(N+1)/2$, and then introduce a passive filtering setup in the mode with $(N-1)/2$ QDs to compensate the loss that is introduced by a practical single-photon scattering process. Therefore, the creation efficiency of N-QD GHZ state is

$$\eta'_{\mathrm{GHZ}} = |R_-|^m = \Big|\frac{r(\Delta, g) - r(\Delta, 0)}{2}\Big|^m. \tag{8}$$

Here $m = 2[(N+1)/2]$, where $[x]$ is the integer value function that rounds the number x down to the nearest integer; $r(\Delta, g)$ and $r(\Delta, 0)$ are reflection coefficients, given by Eqs. (3) and (4).

3.2. Creation of W states of four distant QDs

The main idea for the creation of W-state entanglement among four QDs also exploits the aforementioned single-photon and single-spin interface. We first create single-photon entanglement involving 4 spatial modes, and then impinge the photon in each spatial mode into a QD-cavity system that scatters the photon and creates the correlation between the photon and the QD. After filtering out the error scattering components, the W state of four QDs can be created by eliminating the knowledge of which path the single photon passes, shown in Fig. 3. BS_1 and BS_2 are 50/50 beam splitters; H_1 and H_2 are half-wave plates that complete the Hadamard transformation on photons passing them.

The single photon is initialized to be the linear-polarized state $|\psi\rangle = (|H\rangle + |V\rangle)/\sqrt{2}$ and the four QDs are all in the state $|+\rangle$. The single photon $|\psi\rangle$ under the combined effect of BS_1 and $PBS_{1,2}$ evolves into a single-photon W state $|\psi'\rangle = (|V_1\rangle + |H_2\rangle + |V_3\rangle + |H_4\rangle)/2$, where the four subscripts (i =1, 2, 3, 4) denote the photon in the spatial modes that is scattered by the cavity containing the QD s_i. The photon is then scattered by a QD-cavity system no matter in which spatial mode the photon is. The state of the hybrid system, consisting of the photon and the four

Optics EXPRESS

QDs after the scattering process, evolves into a non-normalized state

$$\begin{aligned}|\Phi_1\rangle = R_-\big(&|H_1\rangle|-\rangle_{s_1}|+\rangle_{s_2}|+\rangle_{s_3}|+\rangle_{s_4} + |V_2\rangle|+\rangle_{s_1}|-\rangle_{s_2}|+\rangle_{s_3}|+\rangle_{s_4}\\ &+ |H_3\rangle|+\rangle_{s_1}|+\rangle_{s_2}|-\rangle_{s_3}|+\rangle_{s_4} + |V_4\rangle|+\rangle_{s_1}|+\rangle_{s_2}|+\rangle_{s_3}|-\rangle_{s_4}\big)\\ &+ R_+|\psi'\rangle|+\rangle_{s_1}|+\rangle_{s_2}|+\rangle_{s_3}|+\rangle_{s_4},\end{aligned} \tag{9}$$

The spatial modes 1 and 2 (3 and 4) of the photon combine at PBS_3 (PBS_4). Note the optical paths of the four individual modes have been tuned to zero. The components in the last line usually lead to errors, and they are passively filtered out by either PBS_3 or PBS_4. The other components will pass the photon through either H_1 or H_2 that completes the Hadamard transformation of the photon.

When a photon is emitted from either output of BS_2, the hybrid system evolves into

$$|\Phi_2\rangle = \frac{1}{2}\big(|H_1\rangle|W_1\rangle + |V_1\rangle|W_2\rangle + |H_2\rangle|W_3\rangle + |V_2\rangle|W_4\rangle\big), \tag{10}$$

where $|W_i\rangle$ (i = 1, 2, 3, and 4) are four W states as follows

$$\begin{aligned}|W_1\rangle &= \frac{1}{2}(\hat{\sigma}_{x_1} + \hat{\sigma}_{x_2} + \hat{\sigma}_{x_3} + \hat{\sigma}_{x_4})|+\rangle_{s_1}|+\rangle_{s_2}|+\rangle_{s_3}|+\rangle_{s_4},\\ |W_2\rangle &= \frac{1}{2}(\hat{\sigma}_{x_2} - \hat{\sigma}_{x_1} + \hat{\sigma}_{x_3} - \hat{\sigma}_{x_4})|+\rangle_{s_1}|+\rangle_{s_2}|+\rangle_{s_3}|+\rangle_{s_4},\\ |W_3\rangle &= \frac{1}{2}(\hat{\sigma}_{x_1} + \hat{\sigma}_{x_2} - \hat{\sigma}_{x_3} - \hat{\sigma}_{x_4})|+\rangle_{s_1}|+\rangle_{s_2}|+\rangle_{s_3}|+\rangle_{s_4},\\ |W_4\rangle &= \frac{1}{2}(\hat{\sigma}_{x_2} - \hat{\sigma}_{x_1} - \hat{\sigma}_{x_3} + \hat{\sigma}_{x_4})|+\rangle_{s_1}|+\rangle_{s_2}|+\rangle_{s_3}|+\rangle_{s_4}.\end{aligned} \tag{11}$$

Here the operator $\hat{\sigma}_{x_i}$ completes the bit-flip transitions of the QD s_i by $|\pm\rangle_{s_i} \leftrightarrow |\mp\rangle_{s_i}$. A measurement of the photon state will project the four-QD system into one of the four W states associating with a particular photon state. Furthermore, these four W states can be converted among each other by using two local phase-flip operations.

The extension of the method to create W states of larger numbers (N) of QDs is also straightforward. We can use more BS and PBS to create a single-photon W state involving N spatial modes that independently interact with N QD-cavity systems. After the scattering process, the correct components introduce a Hadamard transformation on the photon and then interfere at 50/50 BSs to eliminate the information of optical paths in which the photon passes. For instance, to create eight-QD W states, the interference part can be arranged in a similar way as that shown in Fig. 3 for two subsystems that each consists of four QDs, while two additional interference operations are required to eliminate the information of subsystems in which the photon passes. Note that the efficiency of W-state creation is independent of N and

$$\eta'_{\rm W} = |R_-|^2 = \Big|\frac{r(\Delta, g) - r(\Delta, 0)}{2}\Big|^2, \tag{12}$$

because there is only one effective single-photon scattering process, no matter how many QDs are involved. Furthermore, the requirement of multi-path interference in previous protocols are removed [61–65], making our protocol more efficient for W-state creation among distant stationary systems.

4. Performance of multipartite entanglement creation

The effective interface between a single photon and a QD spin constitutes the main building block for the creation of multipartite entanglement. Both of the efficiency and the fidelity of

Optics EXPRESS

our created multipartite entanglement can, in principle, approach unity for ideal scattering in the strong-coupling regime with $\kappa_s \ll \kappa$ and $\gamma, \kappa \ll g$ (or in the high-cooperativity regime with $\kappa_s \ll \kappa$, $\gamma \ll g \ll \kappa$, and $\gamma\kappa \ll g^2$). We use PBSs to passively filter out the error cases caused by deviation from the ideal single-photon scattering condition. In doing so, the fidelity of creating multipartite entanglement remains near-unity even in practical scattering conditions, which is quite different from the conventional schemes [51,55–57]. Unlike the fidelity, the efficiency of creating multipartite entanglement depends on the difference of reflection coefficients $|R_-|$. For instance, the efficiencies of our GHZ-state and W-state creation protocols using a single photon detuned from the cavity mode by Δ are respectively shown in Eqs. (8) and (12) as a function of $|R_-|$. The finite bandwidth of single photon pulses, the finite coupling strength g, and the cavity intrinsic loss κ_s reduce the difference of reflection coefficients $|R_-|$, and thus reduce the creation efficiency. However, in our protocol, we can still achieve a high efficiency for experimentally available parameters.

When single-photon pulses are used in our protocols, the efficiencies of creating GHZ and W states are respectively $\eta_{\rm GHZ} = \int d\Delta f(\Delta)\,\eta'_{\rm GHZ}$ and $\eta_{\rm W} = \int d\Delta f(\Delta)\,\eta'_{\rm W}$ as a function of the input coupling rate κ/κ_s and the QD-cavity coupling rate g/κ_s. Without loss of generality, the single-photon pulse shape with a bandwidth $\sigma_\omega = \gamma$ is assumed to have a Gaussian function $f(\Delta) = \exp[-(\Delta/\sigma_\omega)^2]/\sqrt{\pi}\sigma_\omega$.

We first take parameters $(\kappa_s, \gamma) = (30\ \mu\text{eV}, 0.3\ \mu\text{eV})$ from experimental works [92,93] to show the influence of the input coupling rate κ on the creation efficiencies (see Fig. 4). For existing coupling rates $g/\kappa_s = 1$ and $\kappa/\kappa_s \simeq 3$ [92,93], the efficiencies of creating the four-QD GHZ state and W state are about $\eta_{\rm GHZ} = 0.30$ and $\eta_{\rm W} = 0.55$, respectively. When we fix the coupling rate $g/\kappa_s = 1$, the efficiencies increase to the peak $\eta_{\rm GHZ} = 0.59$ and $\eta_{\rm W} = 0.77$ as the input coupling rate increases to about $\kappa/\kappa_s = 9$. However, when κ/κ_s increases further, both $\eta_{\rm GHZ}$ and $\eta_{\rm W}$ decrease gradually (here $g/\kappa_s = 1$). This is because the increase of κ/κ_s for a fixed g/κ_s leads to two competitive effects on the efficiencies: the decrease of the cooperativity $C = 4g^2/(\kappa + \kappa_s)\gamma$, limiting the probability that a single photon is scattered into the cavity mode, and the increase of a cavity-output amplitude $\kappa/(\kappa_s + \kappa)$ [26], meaning a larger ratio between the useful and loss components. If the input photon pulse has a narrow bandwidth, the efficiencies reach the peaks when $(\kappa/\kappa_s)^2 \sim 4g^2/\kappa_s\gamma + 1$. For a large κ/κ_s, the increase of the QD-cavity coupling rate can also improve the efficiencies $\eta_{\rm GHZ}$ and $\eta_{\rm W}$. For example, when $g/\kappa_s = 2$, the efficiencies remains $\eta_{\rm GHZ} \approx 0.81$ and $\eta_{\rm W} \approx 0.90$ over the region $\kappa/\kappa_s \in (20, 60)$, as shown by the dashed-blue and the solid-magenta curves in Fig. 4. In this region, the two aforementioned competitive effects almost compensate each other for $g/\kappa_s = 2$.

In Fig. 5, we fix κ/κ_s and study the influence of the QD-cavity coupling on the efficiencies. We find that the obtainable efficiencies of the GHZ and W states are both bounded by the cavity-output amplitude $\kappa/(\kappa + \kappa_s)$, which limits the efficiency to collect a photon from the cavity. The maximum efficiency of creating the four-QD GHZ state is $\eta_{\rm GHZ}^{\rm max} = [\kappa/(\kappa_s + \kappa)]^4$ and that for the four-QD W state is $\eta_{\rm W}^{\rm max} = [\kappa/(\kappa_s + \kappa)]^2$. When g is small, the efficiencies of our protocols increase quickly as the QD-cavity coupling rate g/κ_s increases, because the cooperativity C increases as the square of g and thus increases the probability that a single photon is scattered into the cavity mode. However, this probability almost approaches to 1 when $g/\kappa_s = 2$ and $\kappa/\kappa_s = 9$ ($\kappa/\kappa_s = 19$); the efficiency to collect a photon from the cavity for a single-photon scattering process is therefore close to stable value when $g/\kappa_s > 2$. As a result, the efficiencies $\eta_{\rm GHZ}$ and $\eta_{\rm W}$ reach the upper limit 0.81 and 0.90, respectively, and become stable for $g/\kappa_s > 2$.

For a N-QD system, the efficiency of GHZ-state creation is dependent on the qubit number and exponentially decreased for practical scattering. Its maximum efficiency is $[\kappa/(\kappa_s + \kappa)]^{2[(N+1)/2]}$ with $\kappa/(\kappa_s + \kappa) = 0.95$ for a realistic input coupling rate $\kappa/\kappa_s = 19$. For instance, the maximum efficiencies of GHZ-state creation decrease respectively to 0.74 and 0.60, when the qubit number is increased to $N = 6$ and $N = 10$. In contrast, the efficiency of N-QD W-state creation is

Optics EXPRESS

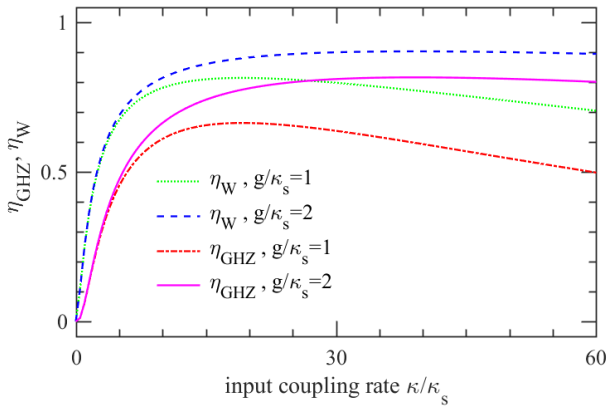

Fig. 4. Efficiencies η_{GHZ} and η_W of the four-QD GHZ-state and W-state creation protocols versus the input coupling rate κ/κ_s for different QD-cavity coupling rates $g/\kappa_s = 1$ and $g/\kappa_s = 2$. Here, $(\kappa_s, \gamma) = (30\ \mu\text{eV}, 0.3\ \mu\text{eV})$. The bandwidth of the input single-photon pulse is $\sigma_\omega = \gamma$.

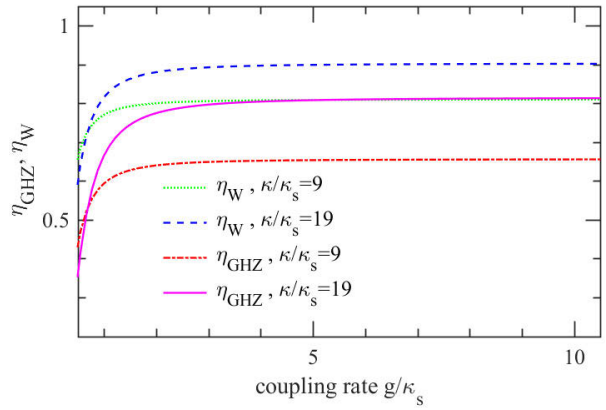

Fig. 5. Efficiencies η_{GHZ} and η_W of the four-QD GHZ-state and W-state creation protocols versus the QD-cavity coupling rate g/κ_s for different input coupling rates $\kappa/\kappa_s = 9$ and $\kappa/\kappa_s = 19$. Other parameters are $(\kappa_s, \gamma) = (30\ \mu\text{eV}, 0.3\ \mu\text{eV})$ and $\sigma_\omega = \gamma$.

independent of the qubit number and its maximum is 0.90 for $\kappa/\kappa_s = 19$, which is identical to that for $N = 4$ with the same parameters.

We have discussed the effect of non-ideal single-photon scattering on the performance of our multipartite-entanglement creation protocols. This non-ideal scattering does not decrease the fidelity of entanglement creation, because all error events involving in a practical scattering process are passively filtered out. In doing so, we convert the photon scattering heralded. Thus, the error events only decrease the efficiency of creating multipartite-entangled states.

The finite coherence time of photons usually plays an important role in single-photon interference. However, its influence on entanglement fidelities can be removed away, when all paths the photon takes in our entanglement creation protocols are tuned to be equal [94]. For charged QDs, the long electron-spin coherence time T_2 of several microseconds has been reported by using spin-echo techniques or by polarizing the nuclei, while the spin-relaxation time T_1 is in the millisecond range that is considerably longer than T_2 [89,95]. In contrast, the time for performing a single-photon scattering process is about $T_0 = 1$ ns, and then the time required

Optics EXPRESS

to create a N-QD GHZ state (W state) is $[N/2]$ ns (1 ns), which is significantly shorter than T_2. Therefore, the decoherence of QDs decreases the entanglement fidelities by an amount of less than 0.01 [76,91], making our protocols faithful for multipartite-entanglement-based quantum tasks.

So far, we assume all QD-cavity systems identical and neglect their nonuniformity, i.e., QDs might be different from each other with the latest advances in microfabrication, and couple differently to their respective cavities [74]. The aforementioned system nonuniformity changes the single-photon probability amplitude in different paths in Figs. 2 and 3, leading to error that decreases the entanglement fidelity. Our proposals can be slightly modified to suppress such error via tuning the single-photon probability amplitude identical in different paths, because the probability amplitude, proportional to R_-s in different paths, can be determined in advance with additional single photons and then modified with passive linear elements. For instance, to filter out the error caused by the system nonuniformity in GHZ-state creation, one can place a BS before PBS_3 in the path with a larger probability amplitude and balance it to match that in the other path in Fig. 2.

5. Discussion and summary

Multipartite entanglement among many distant stationary qubits is useful for both fundamental research and quantum technology application [34–37]. Our protocols for creating GHZ and W states both work in a heralded way that their success is signaled by a click of single-photon detectors. Furthermore, the fidelities of both protocols are robust to the imperfections that are introduced by deviation from the ideal single-photon scattering condition. The error scattering components that decrease the fidelities are converted into heralded errors and are passively filtered out by linear optical elements. The nonuniformity of these QDs and their coupling to the surrounding microcavities is usually a serious problem and decreases the fidelity of entanglement creation processes [55–57,61–64]. Fortunately, the detrimental effect of the nonuniformity in our protocols can be simply suppressed by using passive filters.

In the protocol for the creation of GHZ states, an arbitrary N-QD system is separated into two subgroups that interact with a photon in the reflection or transmission modes of a BS. Therefore, a click of single-photon detectors heralds the success of GHZ-state creation, since this photon flips the state of all QDs in either subspace in an indistinguishable way. The photon amplitudes in both spatial modes are tuned to be equal before the photon enters the interference setup consisting of PBS_3 and H. This is significantly different from protocols that place all stationary qubits in the same spatial mode of the BS [55,56], in which the photon loss due to non-ideal scattering adds up in a higher rate $(1 - |R_-|^{2N})$ other than $(1 - |R_-|^N)$ in the present protocol. In the protocol for the creation of N-QD W-state entanglement, there is only one effective single-photon scattering process involved; the efficiency is a constant η_W that is independent of the number N. We cascade two-spatial-mode interference to eliminate the information of optical paths in which the photon passes. Therefore, the protocol can be easily extended to create W-state entanglement among systems consisting of larger numbers of stationary qubits.

In summary, we have proposed two efficient protocols for creating GHZ and W states of distant stationary qubits. Both protocols are scalable and can be straightforwardly extended to larger scale. Error cases resulted from the system nonuniformity and/or the non-ideal single-photon scattering are totally suppressed by using passive filters. Our protocols may pave the way for applications in long-distance multinode quantum communication and networks.

Optics EXPRESS

Funding

National Key R&D Program of China (2017YFA0303700, 2017YFA0303703, 2019YFA0308704); Natural Science Foundation of Jiangsu Province (BK20180461); National Natural Science Foundation of China (11574145, 11690031, 11874212, 11890700, 11890704, 11904171, 61671279); Fundamental Research Funds for the Central Universities (021314380095).

Disclosures

The authors declare no conflicts of interest.

References

1. J. I. Cirac, A. K. Ekert, S. F. Huelga, and C. Macchiavello, "Distributed quantum computation over noisy channels," Phys. Rev. A **59**(6), 4249–4254 (1999).
2. Y. L. Lim, A. Beige, and L. C. Kwek, "Repeat-until-success linear optics distributed quantum computing," Phys. Rev. Lett. **95**(3), 030505 (2005).
3. L. Jiang, J. M. Taylor, A. S. Sørensen, and M. D. Lukin, "Distributed quantum computation based on small quantum registers," Phys. Rev. A **76**(6), 062323 (2007).
4. W. Qin, X. Wang, A. Miranowicz, Z. Zhong, and F. Nori, "Heralded quantum controlled-phase gates with dissipative dynamics in macroscopically distant resonators," Phys. Rev. A **96**(1), 012315 (2017).
5. H.-K. Lo, M. Curty, and K. Tamaki, "Secure quantum key distribution," Nat. Photonics **8**(8), 595–604 (2014).
6. H.-L. Yin, T.-Y. Chen, Z.-W. Yu, H. Liu, L.-X. You, Y.-H. Zhou, S.-J. Chen, Y. Mao, M.-Q. Huang, W.-J. Zhang, H. Chen, M. J. Li, D. Nolan, F. Zhou, X. Jiang, Z. Wang, Q. Zhang, X.-B. Wang, and J.-W. Pan, "Measurement-device-independent quantum key distribution over a 404 km optical fiber," Phys. Rev. Lett. **117**(19), 190501 (2016).
7. S.-K. Liao, W.-Q. Cai, W.-Y. Liu, L. Zhang, Y. Li, J.-G. Ren, J. Yin, Q. Shen, Y. Cao, Z.-P. Li, F.-Z. Li, X.-W. Chen, L.-H. Sun, J.-J. Jia, J.-C. Wu, X.-J. Jiang, J.-F. Wang, Y.-M. Huang, Q. Wang, Y.-L. Zhou, L. Deng, T. Xi, L. Ma, T. Hu, Q. Zhang, Y.-A. Chen, N.-L. Liu, X.-B. Wang, Z.-C. Zhu, C.-Y. Lu, R. Shu, C.-Z. Peng, J.-Y. Wang, and J.-W. Pan, "Satellite-to-ground quantum key distribution," Nature **549**(7670), 43–47 (2017).
8. S. Pirandola, J. Eisert, C. Weedbrook, A. Furusawa, and S. L. Braunstein, "Advances in quantum teleportation," Nat. Photonics **9**(10), 641–652 (2015).
9. G.-L. Long and X.-S. Liu, "Theoretically efficient high-capacity quantum-key-distribution scheme," Phys. Rev. A **65**(3), 032302 (2002).
10. F.-G. Deng, G. L. Long, and X.-S. Liu, "Two-step quantum direct communication protocol using the Einstein-Podolsky-Rosen pair block," Phys. Rev. A **68**(4), 042317 (2003).
11. J.-Y. Hu, B. Yu, M.-Y. Jing, L.-T. Xiao, S.-T. Jia, G.-Q. Qin, and G.-L. Long, "Experimental quantum secure direct communication with single photons," Light: Sci. Appl. **5**(9), e16144 (2016).
12. W. Zhang, D.-S. Ding, Y.-B. Sheng, L. Zhou, B.-S. Shi, and G.-C. Guo, "Quantum secure direct communication with quantum memory," Phys. Rev. Lett. **118**(22), 220501 (2017).
13. F. Zhu, W. Zhang, Y. Sheng, and Y. Huang, "Experimental long-distance quantum secure direct communication," Sci. Bull. **62**(22), 1519–1524 (2017).
14. R. Qi, Z. Sun, Z. Lin, P. Niu, W. Hao, L. Song, Q. Huang, J. Gao, L. Yin, and G.-L. Long, "Implementation and security analysis of practical quantum secure direct communication," Light: Sci. Appl. **8**(1), 22 (2019).
15. J.-W. Pan, Z.-B. Chen, C.-Y. Lu, H. Weinfurter, A. Zeilinger, and M. Żukowski, "Multiphoton entanglement and interferometry," Rev. Mod. Phys. **84**(2), 777–838 (2012).
16. Y. Gao, H. Zhou, D. Zou, X. Peng, and J. Du, "Preparation of Greenberger-Horne-Zeilinger and W states on a one-dimensional ising chain by global control," Phys. Rev. A **87**(3), 032335 (2013).
17. K. Xia and J. Twamley, "Generating spin squeezing states and Greenberger-Horne-Zeilinger entanglement using a hybrid phonon-spin ensemble in diamond," Phys. Rev. B **94**(20), 205118 (2016).
18. I. Schwartz, D. Cogan, E. R. Schmidgall, Y. Don, L. Gantz, O. Kenneth, N. H. Lindner, and D. Gershoni, "Deterministic generation of a cluster state of entangled photons," Science **354**(6311), 434–437 (2016).
19. X.-L. Wang, L.-K. Chen, W. Li, H.-L. Huang, C. Liu, C. Chen, Y.-H. Luo, Z.-E. Su, D. Wu, Z.-D. Li, H. Lu, Y. Hu, X. Jiang, C.-Z. Peng, L. Li, N.-L. Liu, Y.-A. Chen, C.-Y. Lu, and J.-W. Pan, "Experimental ten-photon entanglement," Phys. Rev. Lett. **117**(21), 210502 (2016).
20. H. Kaufmann, T. Ruster, C. T. Schmiegelow, M. A. Luda, V. Kaushal, J. Schulz, D. von Lindenfels, F. Schmidt-Kaler, and U. G. Poschinger, "Scalable creation of long-lived multipartite entanglement," Phys. Rev. Lett. **119**(15), 150503 (2017).
21. V. Macrì, F. Nori, and A. F. Kockum, "Simple preparation of Bell and Greenberger-Horne-Zeilinger states using ultrastrong-coupling circuit QED," Phys. Rev. A **98**(6), 062327 (2018).
22. Y. Zhou, B. Li, X.-X. Li, F.-L. Li, and P.-B. Li, "Preparing multiparticle entangled states of nitrogen-vacancy centers via adiabatic ground-state transitions," Phys. Rev. A **98**(5), 052346 (2018).

Optics EXPRESS

23. C. Song, K. Xu, H. Li, Y.-R. Zhang, X. Zhang, W. Liu, Q. Guo, Z. Wang, W. Ren, J. Hao, H. Feng, H. Fan, D. Zheng, D.-W. Wang, H. Wang, and S.-Y. Zhu, "Generation of multicomponent atomic Schrodinger cat states of up to 20 qubits," Science **365**(6453), 574–577 (2019).
24. H. J. Kimble, "The quantum internet," Nature **453**(7198), 1023–1030 (2008).
25. T. Northup and R. Blatt, "Quantum information transfer using photons," Nat. Photonics **8**(5), 356–363 (2014).
26. P. Lodahl, S. Mahmoodian, and S. Stobbe, "Interfacing single photons and single quantum dots with photonic nanostructures," Rev. Mod. Phys. **87**(2), 347–400 (2015).
27. A. Reiserer and G. Rempe, "Cavity-based quantum networks with single atoms and optical photons," Rev. Mod. Phys. **87**(4), 1379–1418 (2015).
28. T. Li, A. Miranowicz, X. Hu, K. Xia, and F. Nori, "Quantum memory and gates using a Λ-type quantum emitter coupled to a chiral waveguide," Phys. Rev. A **97**(6), 062318 (2018).
29. N. Sangouard, C. Simon, H. de Riedmatten, and N. Gisin, "Quantum repeaters based on atomic ensembles and linear optics," Rev. Mod. Phys. **83**(1), 33–80 (2011).
30. D. E. Chang, V. Vuletić, and M. D. Lukin, "Quantum nonlinear optics–photon by photon," Nat. Photonics **8**(9), 685–694 (2014).
31. E. Togan, Y. Chu, A. S. Trifonov, L. Jiang, J. Maze, L. Childress, M. V. G. Dutt, A. S. Sørensen, P. R. Hemmer, A. S. Zibrov, and M. D. Lukin, "Quantum entanglement between an optical photon and a solid-state spin qubit," Nature **466**(7307), 730–734 (2010).
32. T.-J. Wang, S.-Y. Song, and G. L. Long, "Quantum repeater based on spatial entanglement of photons and quantum-dot spins in optical microcavities," Phys. Rev. A **85**(6), 062311 (2012).
33. C. Wang, Y. Zhang, and G.-S. Jin, "Entanglement purification and concentration of electron-spin entangled states using quantum-dot spins in optical microcavities," Phys. Rev. A **84**(3), 032307 (2011).
34. R. Horodecki, P. Horodecki, M. Horodecki, and K. Horodecki, "Quantum entanglement," Rev. Mod. Phys. **81**(2), 865–942 (2009).
35. T. Tashima, M. S. Tame, S. K. Özdemir, F. Nori, M. Koashi, and H. Weinfurter, "Photonic multipartite entanglement conversion using nonlocal operations," Phys. Rev. A **94**(5), 052309 (2016).
36. M. Walter, D. Gross, and J. Eisert, "Multi-partite entanglement," arXiv:1612.02437 (2016).
37. H. Yamasaki, A. Pirker, M. Murao, W. Dür, and B. Kraus, "Multipartite entanglement outperforming bipartite entanglement under limited quantum system sizes," Phys. Rev. A **98**(5), 052313 (2018).
38. M. Hillery, V. Bužek, and A. Berthiaume, "Quantum secret sharing," Phys. Rev. A **59**(3), 1829–1834 (1999).
39. S. Schauer, M. Huber, and B. C. Hiesmayr, "Experimentally feasible security check for *n*-qubit quantum secret sharing," Phys. Rev. A **82**(6), 062311 (2010).
40. L. Zhou and Y.-B. Sheng, "Complete logic Bell-state analysis assisted with photonic Faraday rotation," Phys. Rev. A **92**(4), 042314 (2015).
41. Y.-B. Sheng, F.-G. Deng, and G. L. Long, "Complete hyperentangled-Bell-state analysis for quantum communication," Phys. Rev. A **82**(3), 032318 (2010).
42. L. Dong, Y.-F. Lin, C. Cui, H.-K. Dong, X.-M. Xiu, and Y.-J. Gao, "Fault-tolerant distribution of GHZ states and controlled DSQC based on parity analyses," Opt. Express **25**(16), 18581–18591 (2017).
43. J. Ribeiro, G. Murta, and S. Wehner, "Fully device-independent conference key agreement," Phys. Rev. A **97**(2), 022307 (2018).
44. C. F. Roos, M. Riebe, H. Häffner, W. Hänsel, J. Benhelm, G. P. Lancaster, C. Becher, F. Schmidt-Kaler, and R. Blatt, "Control and measurement of three-qubit entangled states," Science **304**(5676), 1478–1480 (2004).
45. H. Häffner, W. Hänsel, C. Roos, J. Benhelm, M. Chwalla, T. Körber, U. Rapol, M. Riebe, P. Schmidt, C. Becher, O. Gühne, W. Dür, and R. S. Blatt, "Scalable multiparticle entanglement of trapped ions," Nature **438**(7068), 643–646 (2005).
46. M. Gräfe, R. Heilmann, A. Perez-Leija, R. Keil, F. Dreisow, M. Heinrich, H. Moya-Cessa, S. Nolte, D. N. Christodoulides, and A. Szameit, "On-chip generation of high-order single-photon W-states," Nat. Photonics **8**(10), 791–795 (2014).
47. B.-S. Shi and A. Tomita, "Teleportation of an unknown state by W state," Phys. Lett. A **296**(4-5), 161–164 (2002).
48. J. Joo, Y.-J. Park, S. Oh, and J. Kim, "Quantum teleportation via a W state," New J. Phys. **5**, 136 (2003).
49. S.-B. Zheng, "Splitting quantum information via W states," Phys. Rev. A **74**(5), 054303 (2006).
50. P. Agrawal and A. Pati, "Perfect teleportation and superdense coding with W states," Phys. Rev. A **74**(6), 062320 (2006).
51. X. Han, S. Hu, Q. Guo, H.-F. Wang, A.-D. Zhu, and S. Zhang, "Effective W-state fusion strategies for electronic and photonic qubits via the quantum-dot-microcavity coupled system," Sci. Rep. **5**(1), 12790 (2015).
52. V. Lipinska, G. Murta, and S. Wehner, "Anonymous transmission in a noisy quantum network using the W state," Phys. Rev. A **98**(5), 052320 (2018).
53. M. Krenn, A. Hochrainer, M. Lahiri, and A. Zeilinger, "Entanglement by path identity," Phys. Rev. Lett. **118**(8), 080401 (2017).
54. N. Bergamasco, M. Menotti, J. E. Sipe, and M. Liscidini, "Generation of path-encoded Greenberger-Horne-Zeilinger states," Phys. Rev. Appl. **8**(5), 054014 (2017).
55. Z. J. Deng, M. Feng, and K. L. Gao, "Preparation of entangled states of four remote atomic qubits in decoherence-free subspace," Phys. Rev. A **75**(2), 024302 (2007).

Optics EXPRESS

56. A. Zheng, J. Li, R. Yu, X.-Y. Lü, and Y. Wu, "Generation of Greenberger-Horne-Zeilinger state of distant diamond nitrogen-vacancy centers via nanocavity input-output process," Opt. Express **20**(15), 16902–16912 (2012).
57. J. Lee, J. Park, S. M. Lee, H.-W. Lee, and A. H. Khosa, "Scalable cavity-QED-based scheme of generating entanglement of atoms and of cavity fields," Phys. Rev. A **77**(3), 032327 (2008).
58. Z. Yan, Y. Liu, J. Yan, and X. Jia, "Deterministically entangling multiple remote quantum memories inside an optical cavity," Phys. Rev. A **97**(1), 013856 (2018).
59. C.-S. Yu, X. X. Yi, H.-S. Song, and D. Mei, "Robust preparation of Greenberger-Horne-Zeilinger and W states of three distant atoms," Phys. Rev. A **75**(4), 044301 (2007).
60. K. S. Choi, A. Goban, S. B. Papp, S. J. Van Enk, and H. J. Kimble, "Entanglement of spin waves among four quantum memories," Nature **468**(7322), 412–416 (2010).
61. J. Song, Y. Xia, and H.-S. Song, "Quantum nodes for W-state generation in noisy channels," Phys. Rev. A **78**(2), 024302 (2008).
62. W. L. Yang, H. Wei, F. Zhou, and M. Feng, "Generation of multi-atom entangled states and implementation of controlled-phase gating using photonic modules," J. Phys. B: At., Mol. Opt. Phys. **42**(5), 055503 (2009).
63. H.-F. Wang, S. Zhang, X. X. Yi, X. Ji, and K.-H. Yeon, "Robust and scalable scheme to generate multipartite atom–photon and atom–atom entangled w states by interference," J. Opt. Soc. Am. B **29**(2), 257–261 (2012).
64. Y.-H. Kang, Y. Xia, and P.-M. Lu, "Effective scheme for preparation of a spin-qubit Greenberger–Horne–Zeilinger state and W state in a quantum-dot-microcavity system," J. Opt. Soc. Am. B **32**(7), 1323–1329 (2015).
65. Y. Pu, Y. Wu, N. Jiang, W. Chang, C. Li, S. Zhang, and L. Duan, "Experimental entanglement of 25 individually accessible atomic quantum interfaces," Sci. Adv. **4**(4), eaar3931 (2018).
66. W. Yang, Z. Xu, M. Feng, and J. Du, "Entanglement of separate nitrogen-vacancy centers coupled to a whispering-gallery mode cavity," New J. Phys. **12**(11), 113039 (2010).
67. T. Liu, Q.-P. Su, S.-J. Xiong, J.-M. Liu, C.-P. Yang, and F. Nori, "Generation of a macroscopic entangled coherent state using quantum memories in circuit QED," Sci. Rep. **6**(1), 32004 (2016).
68. Y.-H. Kang, Y.-H. Chen, Z.-C. Shi, J. Song, and Y. Xia, "Fast preparation of *W* states with superconducting quantum interference devices by using dressed states," Phys. Rev. A **94**(5), 052311 (2016).
69. X. Q. Shao, J. H. Wu, X. X. Yi, and G.-L. Long, "Dissipative preparation of steady Greenberger-Horne-Zeilinger states for Rydberg atoms with quantum Zeno dynamics," Phys. Rev. A **96**(6), 062315 (2017).
70. W. Qin, A. Miranowicz, P.-B. Li, X.-Y. Lü, J. Q. You, and F. Nori, "Exponentially enhanced light-matter interaction, cooperativities, and steady-state entanglement using parametric amplification," Phys. Rev. Lett. **120**(9), 093601 (2018).
71. M. Qurban, M. Ikram, G.-Q. Ge, and M. S. Zubairy, "Entanglement generation among quantum dots and surface plasmons of a metallic nanoring," J. Phys. B: At., Mol. Opt. Phys. **51**(15), 155502 (2018).
72. Z. Yan, Y.-R. Zhang, M. Gong, Y. Wu, Y. Zheng, S. Li, C. Wang, F. Liang, J. Lin, Y. Xu, C. Guo, L. Sun, C.-Z. Peng, K. Xia, H. Deng, Hui Rong, J. Q. You, F. Nori, H. Fan, X. Zhu, and J.-W. Pan, "Strongly correlated quantum walks with a 12-qubit superconducting processor," Science **364**(6442), 753–756 (2019).
73. J. P. Reithmaier, G. Sek, A. Loffler, C. Hofmann, S. Kuhn, S. Reitzenstein, L. Keldysh, V. Kulakovskii, T. Reinecke, and A. Forchel, "Strong coupling in a single quantum dot–semiconductor microcavity system," Nature **432**(7014), 197–200 (2004).
74. I. Buluta, S. Ashhab, and F. Nori, "Natural and artificial atoms for quantum computation," Rep. Prog. Phys. **74**(10), 104401 (2011).
75. C. Y. Hu, A. Young, J. L. O'Brien, W. J. Munro, and J. G. Rarity, "Giant optical faraday rotation induced by a single-electron spin in a quantum dot: applications to entangling remote spins via a single photon," Phys. Rev. B **78**(8), 085307 (2008).
76. C. Y. Hu, W. J. Munro, and J. G. Rarity, "Deterministic photon entangler using a charged quantum dot inside a microcavity," Phys. Rev. B **78**(12), 125318 (2008).
77. J.-H. An, M. Feng, and C. H. Oh, "Quantum-information processing with a single photon by an input-output process with respect to low-Q cavities," Phys. Rev. A **79**(3), 032303 (2009).
78. M. Arcari, I. Söllner, A. Javadi, S. Lindskov Hansen, S. Mahmoodian, J. Liu, H. Thyrrestrup, E. H. Lee, J. D. Song, S. Stobbe, and P. Lodahl, "Near-unity coupling efficiency of a quantum emitter to a photonic crystal waveguide," Phys. Rev. Lett. **113**(9), 093603 (2014).
79. P.-B. Li, Z.-L. Xiang, P. Rabl, and F. Nori, "Hybrid quantum device with nitrogen-vacancy centers in diamond coupled to carbon nanotubes," Phys. Rev. Lett. **117**(1), 015502 (2016).
80. T. Li and F.-G. Deng, "Error-rejecting quantum computing with solid-state spins assisted by low-Q optical microcavities," Phys. Rev. A **94**(6), 062310 (2016).
81. S. Mahmoodian, P. Lodahl, and A. S. Sørensen, "Quantum networks with chiral-light-matter interaction in waveguides," Phys. Rev. Lett. **117**(24), 240501 (2016).
82. D. Buterakos, E. Barnes, and S. E. Economou, "Deterministic generation of all-photonic quantum repeaters from solid-state emitters," Phys. Rev. X **7**(4), 041023 (2017).
83. Z. Liao, M. Al-Amri, and M. S. Zubairy, "Measurement of deep-subwavelength emitter separation in a waveguide-QED system," Opt. Express **25**(25), 31997–32009 (2017).

Optics EXPRESS

84. M. K. Bhaskar, D. D. Sukachev, A. Sipahigil, R. E. Evans, M. J. Burek, C. T. Nguyen, L. J. Rogers, P. Siyushev, M. H. Metsch, H. Park, F. Jelezko, M. Lončar, and M. D. Lukin, "Quantum nonlinear optics with a germanium-vacancy color center in a nanoscale diamond waveguide," Phys. Rev. Lett. **118**(22), 223603 (2017).
85. C. Cao, Y.-W. Duan, X. Chen, R. Zhang, T.-J. Wang, and C. Wang, "Implementation of single-photon quantum routing and decoupling using a nitrogen-vacancy center and a whispering-gallery-mode resonator-waveguide system," Opt. Express **25**(15), 16931–16946 (2017).
86. J.-Z. Liu, N.-Y. Chen, W.-Q. Liu, H.-R. Wei, and M. Hua, "Hyperparallel transistor, router and dynamic random access memory with unity fidelities," Opt. Express **27**(15), 21380–21394 (2019).
87. X. Gu, A. F. Kockum, A. Miranowicz, Y.-X. Liu, and F. Nori, "Microwave photonics with superconducting quantum circuits," Phys. Rep. **718-719**, 1–102 (2017).
88. A. F. Kockum, G. Johansson, and F. Nori, "Decoherence-free interaction between giant atoms in waveguide quantum electrodynamics," Phys. Rev. Lett. **120**(14), 140404 (2018).
89. R. J. Warburton, "Single spins in self-assembled quantum dots," Nat. Mater. **12**(6), 483–493 (2013).
90. M. B. Plenio and P. L. Knight, "The quantum-jump approach to dissipative dynamics in quantum optics," Rev. Mod. Phys. **70**(1), 101–144 (1998).
91. C. O'Brien, T. Zhong, A. Faraon, and C. Simon, "Nondestructive photon detection using a single rare-earth ion coupled to a photonic cavity," Phys. Rev. A **94**(4), 043807 (2016).
92. V. Giesz, N. Somaschi, G. Hornecker, T. Grange, B. Reznychenko, L. De Santis, J. Demory, C. Gomez, I. Sagnes, A. Lemaître, O. Krebs, N. D. Lanzillotti-Kimura, L. Lanco, A. Auffeves, and P. Senellart, "Coherent manipulation of a solid-state artificial atom with few photons," Nat. Commun. **7**(1), 11986 (2016).
93. N. Somaschi, V. Giesz, L. De Santis, J. Loredo, M. P. Almeida, G. Hornecker, S. L. Portalupi, T. Grange, C. Antón, J. Demory, C. Gómez, I. Sagnes, N. D. Lanzillotti-Kimura, A. Lemaítre, A. Auffeves, A. G. White, L. Lanco, and P. Senellart, "Near-optimal single-photon sources in the solid state," Nat. Photonics **10**(5), 340–345 (2016).
94. I. V. Hertel and C. P. Schulz, *Atoms, Molecules and Optical Physics 2* (Springer, 2015).
95. K. De Greve, D. Press, P. L. McMahon, and Y. Yamamoto, "Ultrafast optical control of individual quantum dot spin qubits," Rep. Prog. Phys. **76**(9), 092501 (2013).